Colloid Polym Sci (2006) 284: 947–956
DOI 10.1007/s00396-006-1477-8

ORIGINAL CONTRIBUTION

G. Lagaly
S. Ziesmer

Sol–gel transitions of sodium montmorillonite dispersions by cationic end-capped poly (ethylene oxides) (surface modification of bentonites, IV)

Received: 9 November 2005
Accepted: 15 February 2006
Published online: 28 March 2006

G. Lagaly (✉) · S. Ziesmer
Institute of Inorganic Chemistry,
University Kiel,
24098 Kiel, Germany
e-mail: h.mittag@email.uni-kiel.de
Tel.: +49-431-8807445
Fax: +49-431-8801608

Abstract Poly(ethylene oxides), PEO, end-capped with hexadecyl dimethylammonium, $HDDMA^+$, and trimethylammonium hexyldimethyl-ammonium, THA^{2+}, changed distinctly the sol–gel transition of sodium montmorillonite dispersions. In the presence of $HDDMA^+$-PEO 1,500 and 4,000, domains of sol with increased salt tolerance (c_k=550–1,000 mmol NaCl/l) were found at high polymer and low montmorillonite contents. The corresponding PEO of higher molar mass (20,000 and 35,000) led to extended fields of flocs. THA^{2+}-PEO 1,500 formed attractive gels at polymer concentrations >2–5 g/l and montmorillonite contents >0.5%. These gels showed very high yield values. THA^{2+}-PEO of higher molar mass acted as stabilizing agents. The salt tolerance was highest (300–750 mmol/l) in the presence of THA^{2+}-PEO 20,000. The observed sol–gel diagrams reveal the interplay between polymer end-group fixation on the clay mineral particles, polymer conformation, and colloidal stabilization and destabilization mechanisms.

Keywords Colloidal clay dispersions · Gel · Montmorillonite · Poly(ethylene oxides) · Polymer adsorption · Steric stabilization

Introduction

Colloidal dispersions of bentonites are needed in a broad variety of technical applications such as oil well drilling, foundry molding sands, in the building industry [e.g., subsoil sealing, diaphragma walling, antifriction agents, pipe jacking, additives for concrete, mortar, and tar (bitumen) water emulsions], paints (thickening and anti-settling agents, thixotropy modifiers), cosmetics and pharmaceuticals, and soil improvement [1–9]. The many uses are related to the structure and properties of montmorillonite, the main clay mineral in bentonites. The clay mineral particles are characterized by anisometric particle shape, permanent charges at the faces and variable charges at the edges, ion exchange capacity, intercalation and swelling properties, delamination in water (decomposition of the particles into the single silicate layers), different aggregation modes (band-type or cardhouse-type networks), and thixotropic or antithixotropic flow behavior [2–4, 9–11].

Bentonite dispersions are used as sol, coagulated or flocculated dispersions, or stiffen to gel. Reversible sol–gel transitions are required in many applications, especially in drilling fluids, building industry, and paints. Development of the different colloidal states as a function of salt concentration and montmorillonite content is illustrated by sol–gel diagrams which show the domains of sol, coagulated dispersion, and attractive and repulsive gel (Fig. 1).

Clay mineral dispersions in water or salt solution form two types of gels. The so-called “attractive” gel forms at high salt content when the interaction between the particles is attractive. At low salt concentration and high particle density, the interaction between the particles is repulsive. Formation of the “repulsive” gel is the consequence of the reduced particle mobility due to the overlapping diffuse double layers [13–17].

Practical uses often require changes of the colloidal state, e.g., stiffening a sol, liquefying a gel, or repeptizing a coagulated or flocculated dispersion. This is often achieved by changing the sodium/calcium ratio [1, 2, 11, 12, 18–22].

However, improved and optimized applications, at present and in the future, require a more sensible tailoring of the properties of bentonite dispersions which probably can only be attained by addition of polymers. In this case, the properties of the dispersions are not only determined by the electrostatic and van der Waals forces but also by the polymer–particle interactions, steric stabilization, and depletion effects. The combination of these interactions often makes interpretation of the experimental results difficult but, on the other hand, allows fine tuning of the properties of the dispersions.

For effective steric stabilization, the stabilizing macromolecules must be anchored at the particle surface [10, 23]. Poly(ethylene oxides), PEO, are effective stabilizing macromolecules in aqueous dispersions and can be anchored on clay mineral particles by cationic end groups. We reported before [24] the effect of trimethylammonium end-capped PEO (TMA^+-PEO):

$$(CH_3)_3\overset{\oplus}{N}-(CH_2-CH_2-O)_n-CH_2-CH_2-\overset{\oplus}{N}(CH_3)_3$$
$$TMA^+-PEO$$

on the colloidal state (sol, flocculated, gel) of sodium montmorillonite dispersions. When TMA^+-PEO with a molar mass of about 1,500 (TMA^+-PEO 1,500) was added to sodium montmorillonite dispersions, the sol–gel diagram (polymer concentration vs montmorillonite content) showed a largely extended field of attractive gel. TMA^+-PEO with high molar masses (TMA^+-PEO 20,000 and TMA^+-PEO 35,000) stabilized the dispersions.

The influence of the cationic end-capped PEO should depend on the type of the end groups. When a poly (ethylene oxide) macromolecule with a positive charge at each end is anchored with only one end group at a montmorillonite particle, electrostatic repulsion between the free end groups of neighboring particles can contribute to stabilization. If, however, the end group can anchor at a neighboring particle, bridging reduces the stability of the dispersion, and the particles flocculate or form a gel. Whether the end group remains free or attaches to a neighboring particle should depend on the type of the end group and the availability of free anchoring sites. PEO with different types of end groups illustrate this effect. In addition to TMA^+-PEO, we studied the influence of hexadecyl dimethylammonium ($HDDMA^+$) end groups

$$C_{16}H_{33}(CH_3)_2\overset{\oplus}{N}-(CH_2-CH_2-O)_n-CH_2-CH_2-\overset{\oplus}{N}(CH_3)_2$$
$$C_{16}H_{33}\ HDDMA^+-PEO$$

and trimethylammonium hexyldimethylammonium (THA^{2+}) end groups

$$(CH_2)_3\overset{\oplus}{N}-C_6H_{12}-\overset{\oplus}{N}(CH_2)_2-(CH_2-CH_2-O)_nCH_2-CH_2-\overset{\oplus}{N}(CH_3)_2-C_6H_{12}-\overset{\oplus}{N}(CH_2)_3.$$
$$THA^{2+}-PEO$$

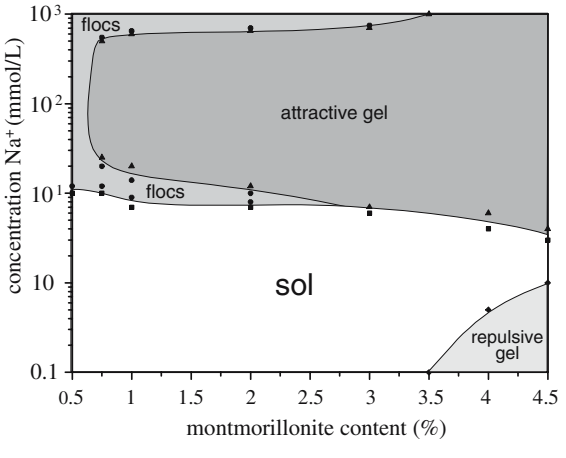

Fig. 1 Sol–gel diagram of sodium montmorillonite dispersions (montmorillonite separated from a Bavarian bentonite)

Experimental

Bentonite

We used a sodium montmorillonite separated from a Bavarian bentonite (Süd-Chemie AG, M 47 in our collection) [24–27]. The layer charge of this montmorillonite determined by alkylammonium exchange [28] was 0.31 eq/mol (charges per formula unit). The total exchange capacity was 1.02 meq/g (= cmol(+)/kg) [29]. This sodium montmorillonite contained about 0.10 meq/g calcium ions.

Modified poly(ethylene oxides)

Starting materials were PEO with nominal molar masses of 1,500, 4,000, 20,000, and 35,000 (Fluka). The terminal OH groups were first replaced by bromine [24, 30, 31]. Reaction with hexadecyl dimethylamine (Fluka) yielded the $HDDMA^+$-PEO [32]. In a similar way were the bromine derivatives reacted with *N*,*N*,*N*′,*N*′-tetramethyl hexyldiamine (Fluka) [32]. The amine was methylated with

Table 1 Cationic poly (ethylene oxides)

PEO	Molar mass expected[1]	Molar mass determined[2]	Charge density (mmol charge (±)/g polymer)[3]
$HDDMA^+$-PEO 1,500[4]	2,164	1,967	1.016
$HDDMA^+$-PEO 4,000	4,664	4,016	0.498
$HDDMA^+$-PEO 20,000	20,664	19,312	0.104
$HDDMA^+$-PEO 35,000	35,664	38,020	0.053
THA^{2+}-PEO 1,500	2,160	1,923	2.080
THA^{2+}-PEO 4,000	4,660	4,319	0.926
THA^{2+}-PEO 20,000	20,660	18,723	0.214
THA^{2+}-PEO 35,000	35,660	37,198	0.108

[1]Calculated from the nominal values of unmodified PEO (Fluka)
[2]By titration of the bromine content
[3]On the basis of the determined molar mass
[4]Error in molar mass reported by Fluka: 1,500±100, 4,000±500, 20,000±3,000, 35,000±3,000

methyl iodide [33]. The counterions of the cationic end groups are bromide ions.

The molar mass of the cationic end-capped PEO ($HDDMA^+$-PEO and THA^{2+}-PEO) were calculated from the bromine content measured by Fajans titration. Evidently, the molar mass of PEO 1,500, 4,000, and 20,000 is slightly smaller than the nominal value, and that of 35,000 is slightly larger (Table 1).

Adsorption isotherms

The polymer adsorption isotherms were determined as described before [24]. The amounts of polymer adsorbed were derived from the carbon content of the slightly washed and vacuum-dried samples. The amounts of exchangeable cations displaced by the THA^{2+} and $HDDMA^+$-PEO 1,500 and 4,000 were measured by atomic adsorption spectroscopy. The small amounts of exchangeable cations displaced by the PEO 20,000 and 35,000 could not be exactly determined.

Flow behavior and sol–gel diagrams

The rheological properties (yield value, viscosity, thixotropy or antithixotropic behavior) were determined as described before [17, 24]. The sol–gel diagrams were constructed on the basis of creeping measurements and visual inspection of the dispersions [17, 24].

Salt tolerance

The salt (NaCl) tolerance of the polymer containing dispersions in the state of sol was derived from the plots of the Bingham yield value vs NaCl concentration and was confirmed by visual inspection of the dispersions in test-tube tests [34]. Whereas test-tube tests of pure sodium montmorillonite dispersions can only be performed at montmorillonite contents <0.1%, the critical coagulation concentration and salt tolerance of sol-type montmorillonite–PEO dispersions could also be measured at higher montmorillonite contents.

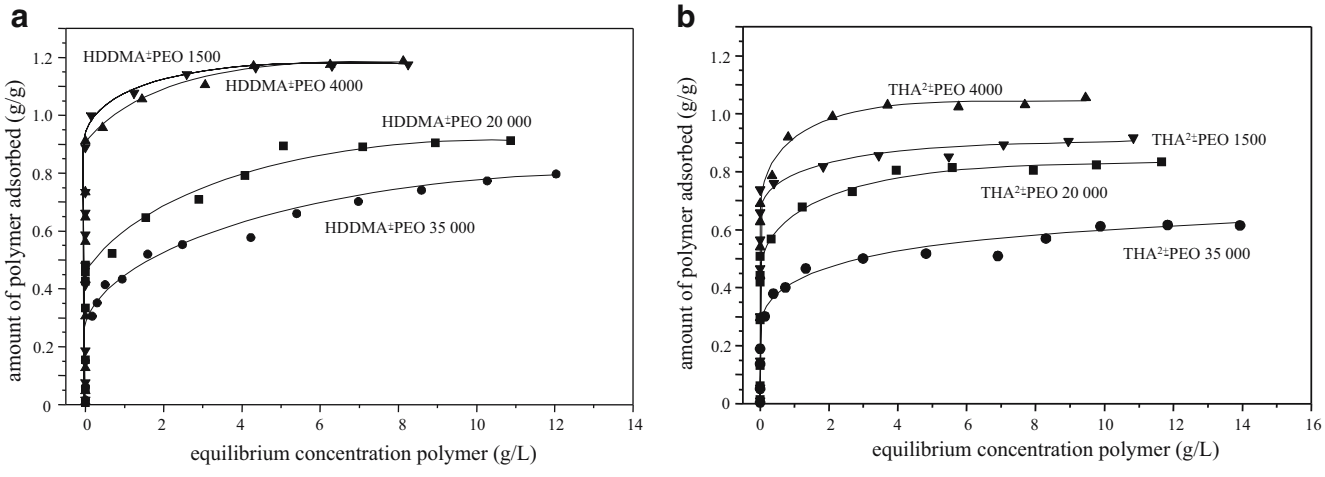

Fig. 2 Adsorption of end-capped poly(ethylene oxides) by sodium montmorillonite, **a** $HDDMA^+$-PEO, **b** THA^{2+}-PEO

Table 2 Maximum amounts of modified poly(ethylene oxides) adsorbed

PEO	Amount adsorbed	
	g/g	mmol/g[1]
TMA^+-PEO 1,500	0.822	0.520
TMA^+-PEO 4,000	0.857	0.194
TMA^+-PEO 20,000	0.689	0.038
TMA^+-PEO 35,000	0.799	0.021
$HDDMA^+$-PEO 1,500	1.169	0.594
$HDDMA^+$-PEO 4,000	1.177	0.293
$HDDMA^+$-PEO 20,000	0.821	0.043
$HDDMA^+$-PEO 35,000	0.770	0.020
THA^{2+}-PEO 1,500	0.905	0.471
THA^{2+}-PEO 4,000	1.036	0.240
THA^{2+}-PEO 20,000	0.821	0.044
THA^{2+}-PEO 35,000	0.615	0.017

Data for TMA^+-PEO for comparison [24]
[1]On the basis of the determined molar masses

Table 3 Bingham yield values τ_B of the 4.5% sodium montmorillonite dispersions in the presence of modified PEO

PEO	τ (Pa) at c_P=0.1 g/l	Minimum		Maximum[1]	
		c_P (g/l)	τ_B (Pa)	c_P (g/l)	τ_B (Pa)
TMA^+-PEO 1,500	4	1	1	40	35[1]
TMA^+-PEO 4,000	8	1	2	12	23.5
TMA^+-PEO 20,000	9	4	1.5	20	6
TMA^+-PEO 35,000	10	10	2	40	11[1]
$HDDMA^+$-PEO 1,500	7	2	2.5	15	45
$HDDMA^+$-PEO 4,000	9	4	2	22	11
$HDDMA^+$-PEO 20,000	10	15	3	40	7.5[1]
$HDDMA^+$-PEO 35,000	11	8	5	40	8.5[1]
THA^{2+}-PEO 1,500	7	1	2	30	145[1]
THA^{2+}-PEO 4,000	9	3	2	15	13.5
THA^{2+}-PEO 20,000	10	20	2	40	9[1]
THA^{2+}-PEO 35,000	10.5	15	5	30	5.5[1]

[1]Yield value τ_B at the highest polymer concentration

Results

Adsorption

All adsorption isotherms of modified PEO indicated a high affinity to the clay mineral (Fig. 2). The plateau values of the $HDDMA^+$ and THA^{2+}-PEO isotherms decreased with increasing molar mass from 0.594 to 0.020 mmol/g ($HDDMA^+$-PEO) and from 0.471 to 0.017 mmol/g (THA^+-PEO) (Table 2). The values for TMA^+-PEO are included in Table 2 for comparison. In all cases, the amounts adsorbed are mainly dependent on the PEO chain length and less on the type of the end group.

$HDDMA^+$-PEO 1,500 and THA^{2+}-PEO 1,500 displaced about 70% of the exchangeable cations, the corresponding PEO 4,000 amounts of 50–60% (at 20 g/l PEO addition).

The basal spacing of the air-dried montmorillonite was 1.15 nm. With increasing amounts of cationic PEO added, it increased to a step at 1.35 nm and reached a plateau at 1.71–1.75 nm (Fig. 3a,b). The spacings were independent on the molar mass with two exceptions: $HDDMA^+$-PEO 1,500 increased the basal spacing to 1.82 nm at high

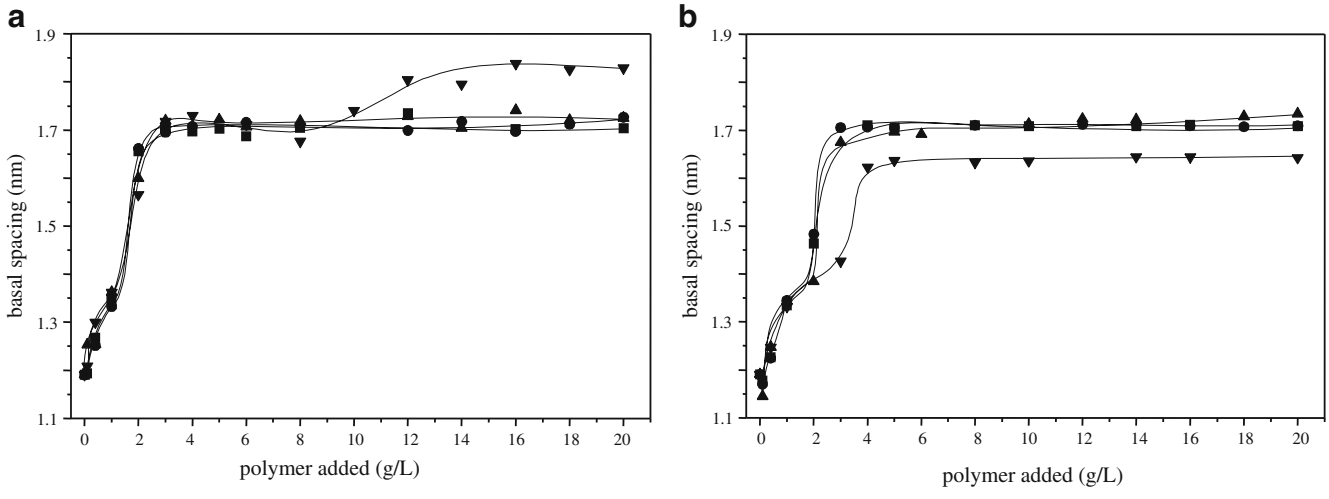

Fig. 3 Basal spacings of air-dried sodium montmorillonite after reaction with modified poly(ethylene oxides), **a** $HDDMA^+$-PEO 1,500 (▾), $HDDMA^+$-PEO 4,000 (▴), $HDDMA^+$-PEO 20,000 (▪), $HDDMA^+$-PEO 35,000 (•), **b** THA^{2+}-PEO 1,500 (▾), THA^{2+}-PEO 4,000 (▴), THA^{2+}-PEO 20,000 (▪), THA^{2+}-PEO 35,000 (•)

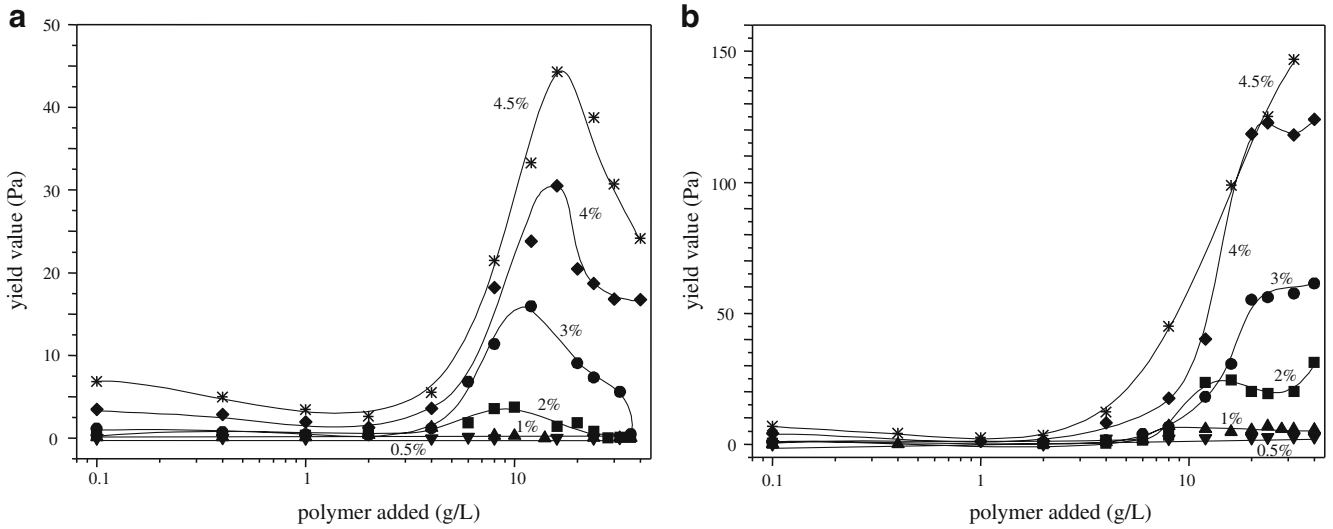

Fig. 4 Bingham yield value of sodium montmorillonite dispersions (0.5–4.5%) in the presence of modified poly(ethylene oxides), **a** $HDDMA^+$-PEO 1,500, **b** THA^{2+}-PEO 1,500

polymer concentration, and THA^{2+}-PEO 1,500 shifted the plateau value to 1.64 nm.

Flow behavior

The Bingham yield value of all PEO–montmorillonite dispersions changed in a similar way (Fig. 4). At 0.1 g/l PEO added, the yield value of the dispersion (4.5% montmorillonite content) increased with the molar mass of PEO from 7 to 11 Pa (for TMA^+-PEO from 4 to 10 Pa). With increasing PEO addition, the yield value decreased to a minimum. The position of this minimum shifted with increasing molar mass from 1 or 2 g/l to 10–20 g/l (Table 3). With further increasing PEO concentration, the yield value raised sharply to a maximum at ≥10 g/l PEO. Very high yield values were observed for $HDDMA^+$-PEO 1,500 and THA^{2+}-PEO 1,500.

The PEO 1,500 and 4,000 provided thixotropic flow behavior to the dispersions at >1% montmorillonite content and polymer concentrations above the minimum of τ_B. $HDDMA^+$ and THA^{2+} 20,000 and 35,000 caused antithixotropic flow.

Sol–gel diagrams

Addition of $HDDMA^+$-PEO to sodium montmorillonite dispersions led to complex sol–gel diagrams. In contrast to TMA^+-PEO 1,500 which forms attractive gels at almost all polymer concentrations >5 g/l [24], large domains of sol and attractive gel developed in the presence of $HDDMA^+$-PEO 1,500 (Fig. 5a). At polymer concentrations <15 g/l, the fields of sol were separated by a field of flocs which, with increasing polymer molar mass, becomes more and more dominant (Fig. 5b–d). This is a striking difference to the behavior of the TMA^+-PEO dispersions which showed pronounced peptization for molar masses of 20,000 and 35,000.

In contrast to the influence of $HDDMA^+$-PEO, the THA^{2+}-PEO yielded simple sol–gel diagrams. THA^{2+}-PEO 1,500 formed an attractive gel phase at all montmorillonite contents and polymer concentrations >3 g/l (Fig. 6a). The THA^{2+}-PEO with higher molar masses were peptizing agents (Fig. 6b–d).

Critical coagulation concentration and salt tolerance

The critical coagulation concentration, c_k, of NaCl for sodium montmorillonite dispersions is about 10 mmol/l when measured in very diluted dispersions. At montmorillonite contents >0.5%, c_k becomes dependent on the solid content [11, 12, 34–37]. The c_k values of the montmorillonite dispersions used in this study were 12 mmol/l NaCl (0.5% montmorillonite) and 8–9 mmol/l for the 1 and 2% dispersions.

The addition of modified PEO increased the salt tolerance[1] in the case of $HDDMA^+$ and THA^{2+}-PEO. High salt tolerance (c_k≥100 mmol/l NaCl) was observed for the sol domains of $HDDMA^+$-PEO 1,500 and 4,000, and THA^{2+}-PEO 4,000 and 20,000 (Table 4). THA^{2+}-PEO

[1] In the case of electrostatic stabilization the influence of salt addition is expressed by the critical coagulation concentration whereas in the case of steric stabilization the term salt resistance or tolerance is more appropriate.

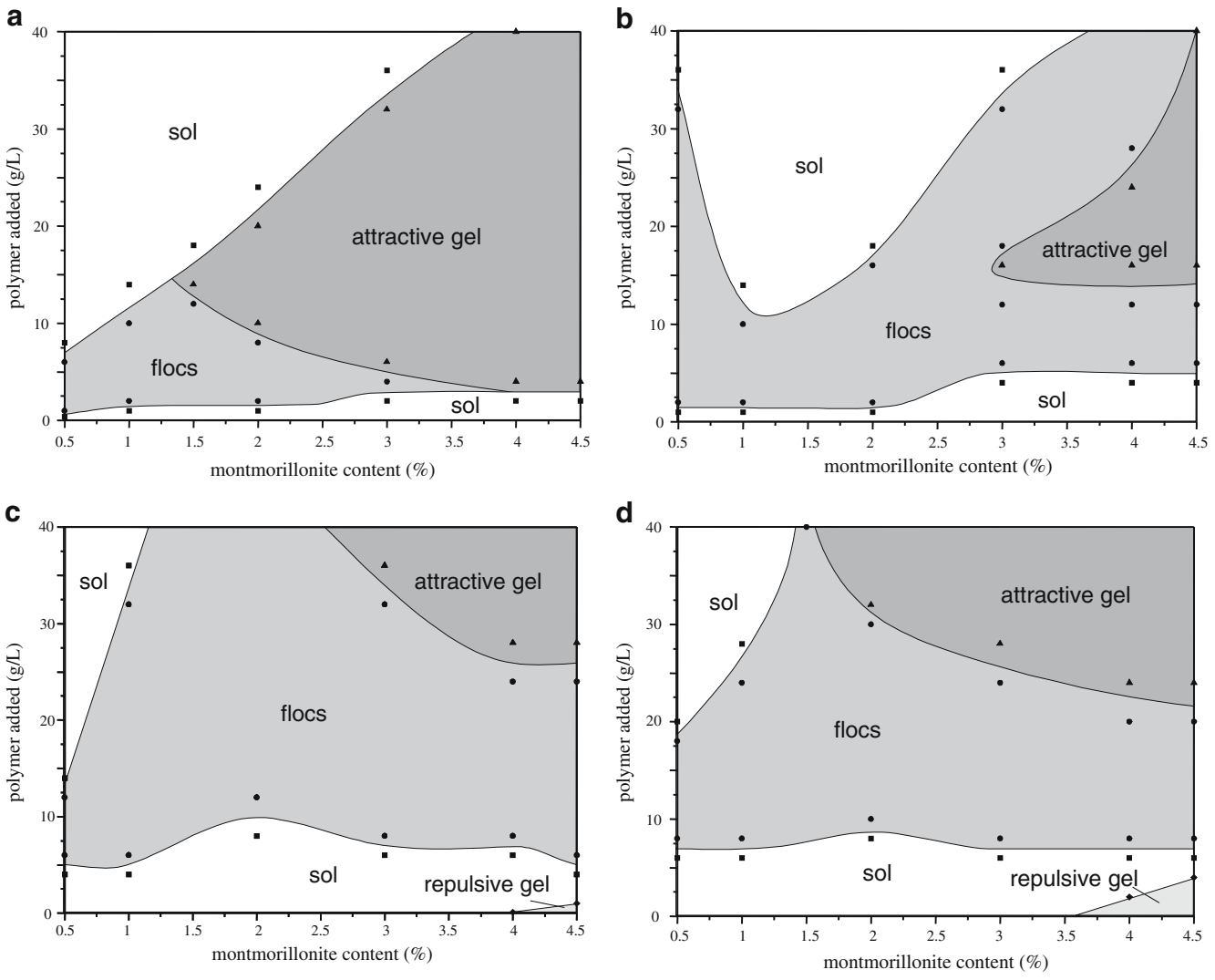

Fig. 5 Sol–gel diagram of sodium montmorillonite dispersions in the presence of $HDDMA^+$-PEO: **a** $HDDMA^+$-PEO 1,500, **b** $HDDMA^+$-PEO 4,000, **c** $HDDMA^+$-PEO 20,000, **d** $HDDMA^+$-PEO 35,000

35,000 peptized the sodium montmorillonite at almost all polymer and montmorillonite contents but the salt tolerance was much smaller than for THA^{2+}-PEO 20,000.

Discussion

Adsorption and aggregation

Sodium montmorillonite particles delaminate in water into the single silicate layers. During the adsorption, the single silicate layers come into contact with the PEO which in the very early steps induce aggregation of most of the layers. Cationic end groups of the PEO are anchored at negative surface sites, however, not forming brushes but mainly train conformations as the consequence of the strong parallel aggregation of the layers. This follows from the basal spacings. They indicate monolayers of PEO segments between the silicate layers at low polymer concentration (basal spacing 1.35 nm) and bilayers (basal spacing 1.75 nm) at higher polymer dosages [24, 38][2]. If the silicate layers were surrounded by the PEO in form of brushes, the polymer-coated layers could not collapse to mono- or bilayer structures during air-drying. As a consequence, the number of adsorbed macromolecules decreases strongly with increasing molar mass so that the total charge of the adsorbed PEO corresponds to only 4% (PEO 20,000) and 2% (PEO 35,000) of the cation exchange capacity. The amounts of PEO adsorbed are

[2] In contrast to the longer chain PEO, the higher number of end groups in the interlayer space increases the plateau value of $HDDMA^+$-PEO 1,500 to 1.82 nm. Contraction to 1.64 nm by THA^{2+}-PEO 1,500 is a consequence of the stronger electrostatic interaction between the divalent end groups and the layer charges.

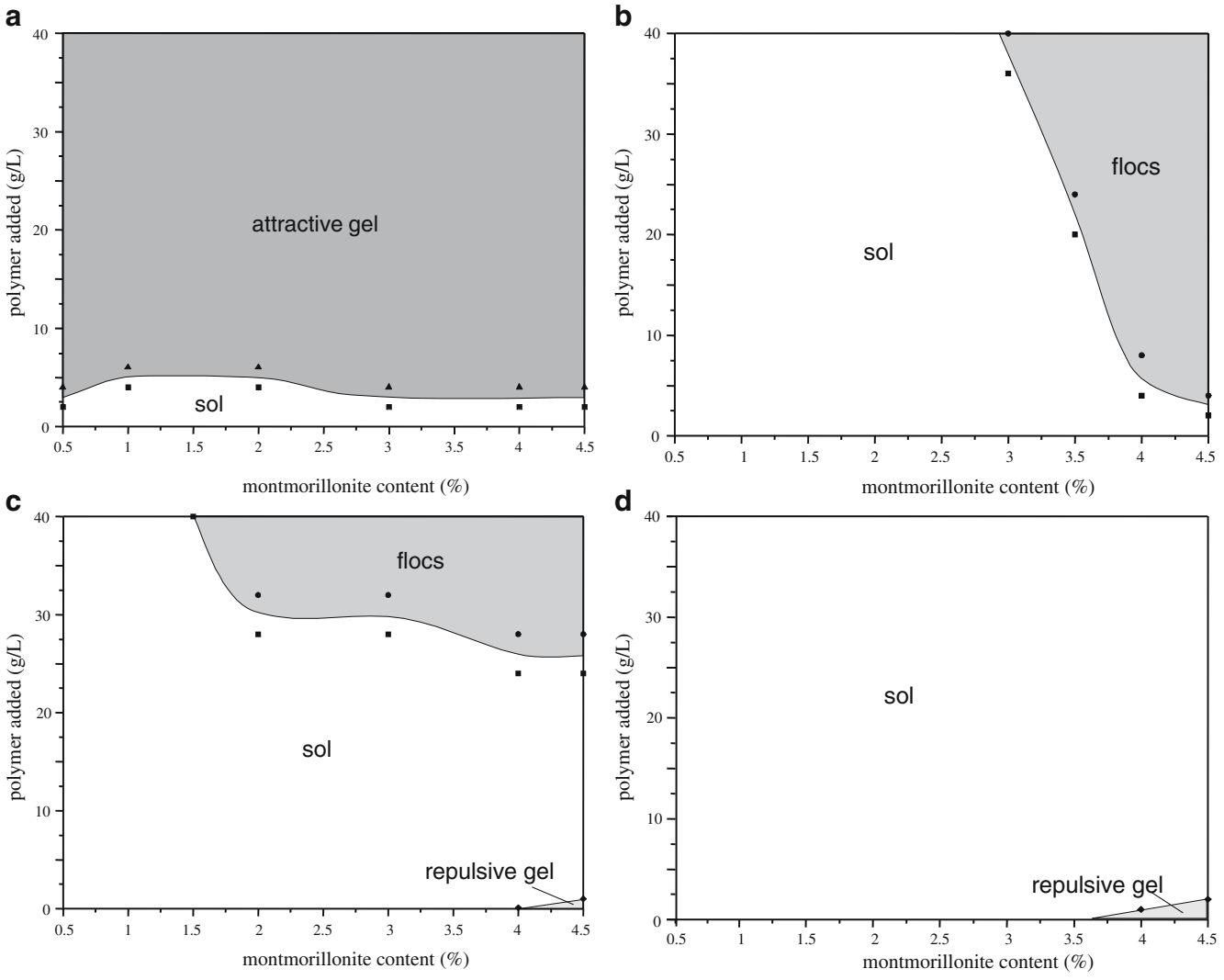

Fig. 6 Sol–gel diagram of sodium montmorillonite dispersions in the presence of THA^{2+}-PEO: **a** THA^{2+}-PEO 1,500, **b** THA^{2+}-PEO 4,000, **c** THA^{2+}-PEO 20,000, **d** THA^{2+}-PEO 35,000

Table 4 Coagulation values c_k for NaCl for sodium montmorillonite dispersions (1% w/w) in the presence of 5–40 g/l modified PEO

PEO	Polymer addition (g/l)				
	5	10	20	30	40
	c_k (mmol NaCl/l)				
TMA^+-PEO 20,000	12	16	25	32	
TMA^+-PEO 35,000	18	24	40	45	
$HDDMA^+$-PEO 1,500			~550	50	25
$HDDMA^+$-PEO 4,000[1]			~1,000	~1,000	20
THA^{2+}-PEO 4,000		50	100		
THA^{2+}-PEO 20,000		~750	~500	~300	
THA^{2+}-PEO 35,000		20	18	20	

Critical coagulation concentration in the absence of polymer 8–9 mmol NaCl/l
[1]2% sodium montmorillonite dispersion

therefore determined by the molar mass and are almost identical for PEO with the same molar mass but different end groups, especially for molar masses 20,000 and 35,000.

When the silicate layers aggregate and include bilayers of PEO, only a part of the ethylene oxide segments can fill the interlayer space. Assuming that the ethylene oxide segments are nearly densely packed in the interlayer space, we calculate that, as in the case of the TMA^+-PEO, about 40–50% of the ethylene oxide units are attached between the silicate layers, and 50–60% of the segments are outside of the particles and can interact with neighboring particles [24]. Thus, addition of the PEO to the delaminated montmorillonite dispersions induce aggregation of the silicate layers in the very early steps of reaction so that clay mineral particles with intercalated bilayers of PEO are formed. The macromolecules protruding out of the

interlayer spaces together with the PEO attached at the external surfaces then stabilize or destabilize these particles in the dispersion medium.

The strong interaction of the modified PEO with the silicate layers is not unexpected. Intercalation of PEO into clay mineral particles has often been reported [38–55]. An important contribution is the strong van der Waals interaction of the ethylene oxide segments with the silicate layer because the CH_2–CH_2–O units like the alkyl chains fit very well the arrangement of the surface oxygen atoms (cf. Fig. 5 in [56]). This strong interaction is the reason that the adsorption does not exceed the formation of bilayers, i.e., formation of poly(ethylene oxide) monolayers on the internal surfaces.

Sol, gel, flocs

At lower montmorillonite contents (<1.5%), the addition of $HDDMA^+$-PEO 1,500 leads to the sequence of colloidal states: sol–coagulation–restabilization (Fig. 5a). Small amounts of $HDDMA^+$-PEO 1,500 coagulate the dispersion in the form of flocs. As only the external surface charges must be compensated by the adsorbed counterions, destabilization does not need an amount of cationic end groups equivalent to the cation exchange capacity but starts at distinctly smaller amounts. Increasing polymer addition causes restabilization, not only by recharging but also by steric stabilization (charge reversal of the $HDDMA^+$-PEO-covered particles is indicated by the electrophoretic mobility [57]). It is interesting that this type of restabilization was not observed for TMA^+-PEO 1,500. The reason may be that the interaction between the hydrophobic hexadecyl groups leads to a larger number of stabilizing polymer loops (Fig. 7). A similar model was proposed by Volpert et al. [58].

The free end groups (i.e., the end groups not bound to a particle by cation exchange) can anchor at neighboring particles if the macromolecules can span the distance. The sol therefore transforms in an attractive gel at higher montmorillonite content (Fig. 5a). The maxima of the yield value (Fig. 4, Table 3) were found in the middle of the gel fields. Increasing concentration of free polymer will reduce bridging, and a denser packing of the particles is required for gel formation. Thus, the field of attractive gel expands with increasing montmorillonite and polymer content (Fig. 5a). On the other hand, the polymer concentration needed for the floc–gel transition decreases with increasing particle density.

The hydrophobic $HDDMA^+$ end groups are responsible that, in contrast to the influence of TMA^+-PEO, increasing molar mass does not stabilize the dispersion but increases the domain of flocs on the extent of sol and gel (Fig. 5b–d). Increasing chain length promotes the anchoring of the hydrophobic end groups at neighboring particles. The hexadecyl moiety then renders the particle surface hydrophobic so that voluminous flocs are formed, comparable to the flocculation by hexadecylammonium ions [4, 10, 59]. Attractive gels are formed only at high polymer and montmorillonite content which could be a consequence of depletion destabilization in the presence of high concentrations of dissolved PEO. The highest yield values are found in these fields of attractive gels (Table 3).

The divalent end groups of the THA^{2+}-PEO distinctly change the sol–gel transitions (Fig. 6a–d). Like TMA^+-PEO 1,500, THA^{2+}-PEO 1,500 leads to the formation of an attractive gel, mainly by bridging the particles, even at low montmorillonite contents. The strong electrostatic anchoring of the divalent end groups to the surface charges leads to gels with very high yield values (Fig. 4b, Table 3). Addition of relatively small amounts (4 g/l) of THA^{2+}-PEO 1,500 to sodium montmorillonite dispersions immediately yields very stiff rigid gels, even at montmorillonite contents of 0.5%.

Higher molar mass THA^{2+}-PEO show a strong peptizing effect. The pronounced peptization is a consequence of the

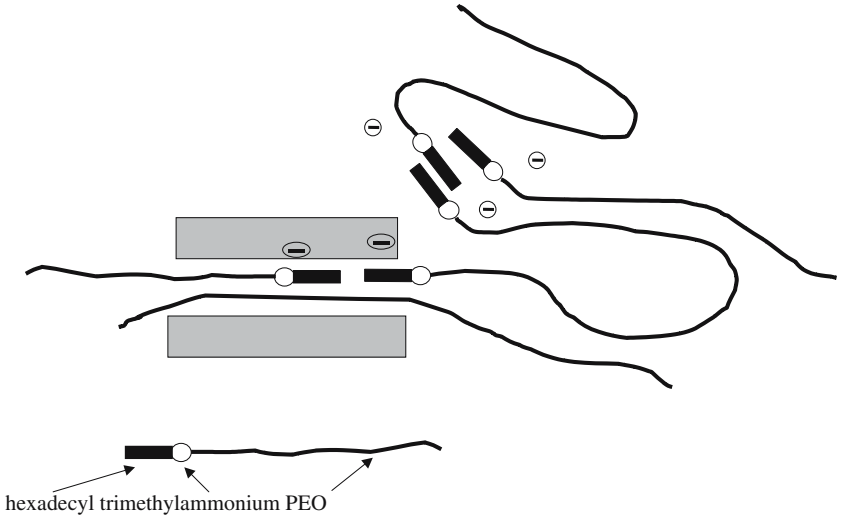

Fig. 7 Formation of loops by aggregating hydrophobic moieties of $HDDMA^+$-PEO

stronger electrostatic interaction between the divalent end groups and the negative particle charges. This interaction could promote the formation of loops when both ends of the PEO attach to the same particle and therefore stabilize the dispersion but could also promote bridging and destabilization of the dispersion. The pronounced sol domains in the diagrams reveal that the first effect is dominant. The domains of flocs in the presence of THA^{2+}-PEO 4,000 and 20,000 may be caused by depletion effects (Fig. 6b,c).

Stability against salt addition

The coagulation concentration and salt tolerance (Table 4) clearly indicate a pronounced influence of the electrostatic besides steric stabilization. The coagulation between montmorillonite particles is initiated by edge(−)/face(−) interaction [4, 10–12, 36, 37]. Free positive end groups of the PEO can anchor at negative sites on the basal plane surfaces of the particles when the distance between neighboring particles is reduced by even small salt additions so that the macromolecules can span the distance [12, 60–63]. This electrostatic interaction then dominates the steric stabilization, and the coagulation concentrations are only slightly enhanced to ≤50 mmol/l NaCl. The system may therefore be considered as an example of limited steric stabilization of dispersions displaying deviant behavior [64].

Steric stabilization appears to be effective when, as discussed above, the PEO chains form loops so that both cationic end groups are attached to the same particles. In these cases, the salt tolerance is distinctly increased to maximum values between 100 and 1,000 mmol/l NaCl. The reduced salt tolerance in the presence of THA^{2+}-PEO 35,000 indicates that the risk of bridging destabilization by very long chains competes with steric stabilization due to formation of loops.

Conclusion

Cationic and anionic PEO change the colloidal states (sol, coagulated, flocculated, attractive and repulsive gel) of sodium montmorillonite dispersions. The influence of the modified PEO reveals the sensible interplay between montmorillonite–PEO interaction, polymer conformation (loops, trains, and tails), and the different colloidal stabilization (electrostatic and steric) and destabilization (charge neutralization, bridging, and depletion) mechanisms. Whereas $HDDMA^{+}$-PEO maintain the sol state of sodium montmorillonite only at lower molar masses (1,500 and 4,000) and not too high montmorillonite contents, THA^{2+}-PEO with molar masses ≥4,000 stabilize the montmorillonite dispersion. The effect of cationic end-capped PEO provides new possibilities for improved applications of bentonites.

References

1. Grim RE (1962) Applied clay mineralogy. McGraw-Hill, New York
2. van Olphen H (1977) An introduction to clay colloid chemistry, 2nd edn. Wiley, New York
3. Lagaly G, Fahn R (1983) In: Ullmanns Enzyclopädie der Technischen Chemie, vol 23, 4th edn. Verlag Chemie, Weinheim, pp 311–326
4. Jasmund K, Lagaly G (eds) (1993) Tonminerale und Tone. Struktur, Eigenschaften, Anwendung und Einsatz in Industrie und Umwelt. Steinkopff Verlag, Darmstadt
5. Murray HH (1986) Clays. In: Ullmann's encyclopedia of industrial chemistry, vol A7. VCH, Weinheim, pp 109–136
6. Murray HH (1999) Clay Miner 34:39
7. Murray HH (2000) Appl Clay Sci 17:207
8. Murray HH (2003) In: Dominguez EA, Mas GR, Cravero F (eds) A clay odyssey. Proceedings of the 12th international clay conference 2001, Bahia Blanca. Elsevier, Amsterdam, pp 3–14
9. Harvey C, Lagaly G (2006) In: Bergaya F, Theng BKG, Lagaly G (eds) Handbook of clay science, chapter 10.1. Elsevier, Amsterdam, pp 507–548
10. Lagaly G, Schulz O, Zimehl R (1997) Dispersionen und Emulsionen. Eine Einführung in die Kolloidik feinverteilter Stoffe einschließlich der Tonminerale. Mit einem historischen Beitrag über Kolloidwissenschaftler von Klaus Beneke. Steinkopff Verlag, Darmstadt, Germany
11. Lagaly G (2005) In: Stechemesser H, Dobias B (eds) Coagulation and flocculation, 2nd edn. Surfactant science series, vol 126, CRC Press, Taylor and Francis Group, LLC, Boca Raton, FL, USA, pp 519–600
12. Lagaly G (2006) In: Bergaya F, Theng BKG, Lagaly G (eds) Handbook of clay science, chap 5. Elsevier, Amsterdam, pp 143–248
13. Callaghan IC, Ottewill RH (1974) Faraday Discuss 57:110
14. Rand B, Pekenć E, Goodwin JW, Smith RW (1980) J Chem Soc Faraday I 76:225
15. Güven N (1992) In: Güven N, Pollastro RM (eds) Clay–water interface and its rheological implications. CMS workshop lectures, vol 4. The Clay Minerals Society, Boulder, CO, USA, pp 82–125
16. Permien T, Lagaly G (1994a) Clay Miner 29:751
17. Abend S, Lagaly G (2000) Appl Clay Sci 16:201
18. Tombácz E, Balász J, Lakatos J, Szántó F (1989) Colloid Polym Sci 267:1016
19. Brandenburg U, Lagaly G (1988) Appl Clay Sci 3:263
20. Lagaly G (1989) Appl Clay Sci 4:105
21. Permien T, Lagaly G (1994b) Clay Miner 29:761
22. Permien T, Lagaly G (1995) Clays Clay Miner 43:229
23. Napper DH (1983) Polymeric stabilization of colloidal dispersions. Academic, London
24. Lagaly G, Ziesmer S (2005) Clay Miner 40:523
25. Tributh H, Lagaly G (1986a) GIT-Fachz Lab 30:524

26. Tributh H, Lagaly G (1986b) GIT-Fachz Lab 30:771
27. Carrado KA, Bergaya F, Decarreau A, Lagaly G, Petit S (2006) In: Bergaya F, Theng BKG, Lagaly G (eds) Handbook of clay science, chap 4. Elsevier, Amsterdam, pp 117–141
28. Lagaly G (1994) In: Mermut A (ed) Charge characteristics of 2:1 clay minerals. CMS workshop lectures, vol 6, The Clay Minerals Society, Boulder, CO, USA, pp 1–46
29. Ammann L, Bergaya F, Lagaly G (2006) Clay Min 40:441–453
30. Bückmann AF, Morr M, Johansson G (1981) Makromol Chem 182:1379
31. Dau J, Lagaly G (1998) Croat Chem Acta 71:983
32. Parreira HC, Lukenbach ER, Lindemann MKO (1979) J Am Oil Chem Soc 56:1015
33. Berardelli ML, Biondi C, De Rossi M, Fonseca G, Giomini M (1972) J Electrochem Soc 119:114
34. Penner D, Lagaly G (2001) Appl Clay Sci 19:131
35. Permien T, Lagaly G (1994c) Colloid Polym Sci 272:1306
36. Lagaly G, Ziesmer S (2003) Adv Colloid Interf Sci 100–102:105
37. Penner D, Lagaly G (2000) Clays Clay Miner 48:24635
38. Parfitt RL, Greenland DJ (1970a) Clay Miner 8:305
39. Parfitt RL, Greenland DJ (1970b) Clay Miner 8:317
40. Zhao X, Urano K, Ogasawara S (1989) Colloid Polym Sci 267:899
41. Ruiz-Hitzky E, Aranda P (1990) Adv Mater 2:545
42. Aranda P, Ruiz-Hitzky E (1992) Chem Mater 4:1395
43. Aranda P, Ruiz-Hitzky E (1999) Appl Clay Sci 15:119
44. Aranda P, Galvan JC, Casal B, Ruiz-Hitzky E (1992) Electrochim Acta 37:1573
45. Ruiz-Hitzky E (1993) Adv Mater 5:334
46. Ruiz-Hitzky E, Aranda P, Casal B, Galvan JC (1995) Adv Mater 7:180
47. Billingham J, Breen C, Yarwood J (1997) Vibr Spectrosc 14:19
48. Breen C, Rawson JO, Mann BE, Aston M (1998) Colloids Surf A 132:17
49. Breen C, Thompson G, Webb M (1999) J Mater Chem 9:3159
50. Bujdák J, Hackett E, Giannelis EP (2000) Chem Mater 12:2168
51. Smalley MV, Hatharasinghe HLM, Osborne I, Swenson J, King SM (2001) Langmuir 17:3800
52. Strawhecker KK, Manias E (2003) Chem Mater 15:844
53. Deng Y, Dixon JB,White GN (2003) Clays Clay Miner 51:150
54. Sonon LS, Thompson ML (2005) Clays Clay Miner 53:45
55. Deng Y, Dixon JB, Whitw GN (2006) Colloid Polym Sci 284:347
56. Lagaly G, Weiss A (1971) Kolloid-Z Z Polym 243:48
57. Ziesmer S (2002) Thesis, University Kiel
58. Volpert E, Selb J, Candau F, Green N, Argillier JF, Audibert A (1998) Langmuir 14:1870
59. Janek M, Lagaly G (2003) Colloid Polym Sci 281:293
60. Kim HS, Lamarche C, Verdier A (1983) Colloid Polym Sci 261:64
61. Lagaly G (1986) In: Ullmann's encyclopedia of industrial chemistry. VCH Verlagsgesellschaft, Weinheim, A7, pp 341–367
62. Lagaly G (2000) In: Ullmann's encyclopedia of industrial chemistry, chap 4, 6th edn. Electronic Release 2000, Wiley, VCH
63. Smith JN, Meadows J, Williams PA (1996) Langmuir 12:3773
64. Napper DH (1983) Polymeric stabilization of colloidal dispersions. Academic, London